

## Full Paper

# Silver nanoparticles as an antimicrobial agent: A case study on *Staphylococcus aureus* and *Escherichia coli* as models for Gram-positive and Gram-negative bacteria

(Received July 12, 2016; Accepted July 18, 2016; J-STAGE Advance publication date: January 24, 2017)

Eman Zakaria Gomaa\*

Department of Biological and Geological Sciences, Faculty of Education, Ain Shams University, Cairo, Egypt

The current research was focused on the characterization and antimicrobial activity of silver nanoparticles (AgNPs) produced by *Bacillus licheniformis* NM120-17. The synthesis was initially observed by a colour change from pale yellow to brown which was further confirmed by UV-Vis spectroscopy. The AgNPs were characterized using TEM, EDAX and FTIR. The synthesized nanoparticles were found to be spherical and uniformly distributed with a size in the range of 9–27.5 nm. The antibacterial activities and acting mechanism of AgNPs were studied with respect to *Staphylococcus aureus* and *Escherichia coli* by measuring the growth curves, protein and reducing sugar leakage, respiratory chain dehydrogenase activity, as well as the formation of bactericidal reactive oxygen species (ROS). The experimental results indicated that 50 mg/ml AgNPs could completely inhibit the growth of bacterial cells and destroy the permeability of bacterial membranes and depress the activity of some membranous enzymes, which cause bacteria to die eventually. These non-toxic nanomaterials, which can be prepared in a simple and cost-effective manner, may be suitable for the formulation of new types of bactericidal materials.

**Key Words:** antibacterial activity; *Escherichia coli*; silver nanoparticles (AgNPs); *Staphylococcus*

## Introduction

Nanotechnology research is emerging as a cutting edge technology which is interdisciplinary with physics, chemistry, biology, materials science and medicine (Narayanan

and Sakhivel, 2010). Their extremely small size and large surface area relative to their volume makes them useful for applications in various fields, such as antibacterials (Souza et al., 2004), therapeutics (Wang et al., 2011), cosmetics, microelectronics (Tomsic et al., 2009), conductive inks and adhesives (Akaijhe et al., 2011).

Silver nanoparticles (AgNPs) are commonly synthesized by chemical reduction (Peterson et al., 2007), irradiation (Shao and Yao, 2006) and laser ablation (Tsuji et al., 2002), which are low yield, energy-intensive, difficult to scale up, often producing high levels of hazardous wastes, and may require the use of organic solvents and toxic reducing agents (Wani et al., 2013). The green synthesis of nanoparticles has gained significant importance in recent years and has become one of the most preferred methods for obtaining biocompatible, cost-effective, clean, non-toxic, easily scaled up for large-scale synthesis, and ecofriendly size-controlled nanoparticles (Dobrucka and Dlugaszewska, 2015). Various bacteria (Chaudhari et al., 2012; Saifuddin et al., 2009), fungi (Gade et al., 2008; Vigneshwaran et al., 2007) and plant sources (Masurkar et al., 2011; Raut et al., 2010) have been used to achieve the green synthesis of silver nanoparticles.

The development of resistant, or even multiresistant, pathogens has become a major problem (Schaller et al., 2004). The investigations on the antibacterial activity of silver nanoparticles have increased (Durán et al., 2010; Gade et al., 2008). In this paper, *S. aureus* and *E. coli* strains were selected as models for Gram-positive and Gram-negative bacteria to understand the antibacterial activity and the acting mechanism of AgNPs produced by *B. licheniformis* NM120-17 at cellular and subcellular levels.

## Materials and Methods

**Bacterial strains and reagents.** All chemicals and media

\*Corresponding author: Eman Zakaria Gomaa, Department of Biological and Geological Sciences, Faculty of Education, Ain Shams University, Cairo, Egypt.

E-mail: emann7778@yahoo.com

None of the authors of this manuscript has any financial or personal relationship with other people or organizations that could inappropriately influence their work.

used were of the purest grade and purchased from Sigma-Aldrich. The test organisms used for antibacterial assay were *Bacillus subtilis* NCTC10400, *Bacillus cereus* ATCC1589, *Staphylococcus aureus* ATCC29213, *Klebsiella pneumonia* ATCC10031, *Salmonella typhi* NCIMB9331, *Escherichia coli* ATCC10536 and *Pseudomonas aeruginosa* ATCC10145 as indicator strains. All these strains were obtained from the Fermentation Biotechnology and Applied Microbiology (FERM-BAM) Centre, Al-Azhar University, Cairo, Egypt. The bacterial strains were maintained by subculturing periodically on nutrient agar and preserved at 4°C prior to use. All solutions were made using ultra-filtered high-purity deionized water.

#### **Isolation and screening of AgNPs producing bacteria.**

A total of 17 different rhizospheric soil samples of maize, wheat and rice were collected from agricultural fields of Cairo, Kaluobia, Giza, Helwan, and Dakahlia governorates (Gomaa, 2012). A sample (1 g) was suspended in 100 ml of 50 mM phosphate buffer (pH 7.0), serially diluted in the same buffer, and plated on LB agar containing (g/l): tryptone, 10; yeast extract, 5; NaCl, 10 and agar, 15) (Kalimuthu et al., 2008). The plates were incubated at 37°C for 2–3 days. After the incubation period, the bacterial colonies were further sub-cultured in the same medium to obtain pure colonies, which were isolated and stored at –80°C.

Screening of silver-nanoparticle-producing bacteria was carried out according to the method described by Gurunathan et al. (2009). Briefly, bacterial isolates were first grown aerobically at 37°C in LB media for 24 h. The cells were harvested by centrifugation at 10,000 × g for 20 min, and resuspended in sterile LB medium to obtain an optical density of 1.0 at 600 nm (OD<sub>600</sub>). After incubation, the culture was centrifuged (10,000 × g 20 min) and the supernatant was mixed with 1 mM silver nitrate in a 1:1 ratio. The final pH of the reaction mixture was adjusted to 8.5 (Darroudi et al., 2010; Deepak et al., 2011). The resultant solutions were kept under shaking conditions (200 rpm) at 37°C under dark conditions till a color change from pale yellow to dark brown was observed.

**Strain identification.** One isolate showing the effective synthesizer of AgNPs was identified by 16S rRNA sequencing according to the method of Rochelle et al. (1995). The gene sequencing was done by Macrogen (South Korea). DNA sequences were aligned using Gene Mapper® v.4.1 and Data Collection v.3.1 Communication Patch1. Bacterial 16S rRNA gene was amplified using the following universal primers for eubacteria: forward primer 27 F (5'-AGAGTTTGATCMTGGCTCAG-3') and reverse primer 1492R (5'-TACGGYTACCTTGTTACGACTT-3'). Sequencing was performed by using Big Dye terminator cycle sequencing kit (Applied BioSystems). Sequencing products were resolved on an Applied Biosystems model 3730XL automated DNA sequencing system (Applied BioSystems). Sequence analysis was performed with sequences in the National Center for Biotechnology Information (NCBI), USA, database using the Basic Local Alignment Search Tool for Nucleotides (BLASTN), (Altschul et al., 1997).

#### **Characterization techniques.**

**UV-visible spectral analysis:** Synthesized silver nanoparticles were further confirmed by UV-visible spectral analysis using a Cary 5000 UV-Vis-NIR spectrophotometer (Varian, Australia).

**Particle size:** Particle size distributions of these samples were also obtained using Zeta sizer Nano ZS (Malvern Instruments, Southborough, UK) using a detection angle of 90° and a 60 mW He-Ne laser operating at a wavelength of 633 nm.

**Transmission Electron Microscopy (TEM) and Energy Dispersive X-ray Spectra (EDX) analysis:** The studies on morphology, size and the distribution of nanoparticles were performed by using a Transmission Electron Microscope (Tecnaï G20, Super twin, double tilt, FEI, The Netherlands). TEM analysis was performed by using a PHILIPS CM 200 instrument operated at an accelerating voltage of 200 kV with a resolution of 0.23 nm. The EDX analysis was carried out using JEOL JSM 7600F.

**X-ray diffraction and Fourier-transform infrared spectroscopy analysis (FT-IR):** The formation and quality of compounds were checked by an X-ray diffraction (XRD) spectrum. FT-IR (Perkin Elmer Spectrum, Jasco-6100) was used to identify the biomolecules associated with the synthesis of silver nanoparticles mediated by bacteria. The dried silver nanoparticles were ground with KBr pellets and measured in the wavelength range 4000 to 400 cm<sup>-1</sup>.

**Antimicrobial activity of silver nanoparticles.** The silver nanoparticles were checked for their antibacterial efficiency using the agar well diffusion assay method (Perez et al., 1990). Each experiment was carried out in triplicate and the mean diameter of the inhibition zones was recorded.

**Bacterial growth curves and MIC determination.** The growth of bacteria exposed to various concentrations of AgNPs powder (0, 25, 50 and 100 mg/ml) was measured for 16 h by taking the readings of the optical density (OD) at 600 nm at 2 h intervals. The minimum inhibitory concentration (MIC) of AgNPs was determined using the plate count method (Magana et al., 2008). The MIC values were interpreted as the highest dilution (lowest concentration) of the sample which showed no growth.

**Effect of AgNPs on the leakage of protein and reducing sugars from bacterial cell membranes.** The leakage of proteins and reducing sugars through membranes was determined. The concentration of AgNPs was adjusted to 50 mg/ml, and the concentration of bacterial cells was 10<sup>5</sup> CFU/ml. Each culture was incubated in a shaking incubator at 37°C for 6 h. Control experiments were conducted without AgNPs. The proteins and reducing sugars were determined by the methods described by Lowry et al. (1951) and Miller (1959), respectively.

**Effect of AgNPs on the enzymatic activity of respiratory chain dehydrogenases.** The dehydrogenase activity was determined according to the method of Iturriaga et al. (2001). Under physiological conditions, colorless idonitrotetrazolium chloride (INT) is reduced by the bacterial respiratory chain dehydrogenase to a dark red wa-

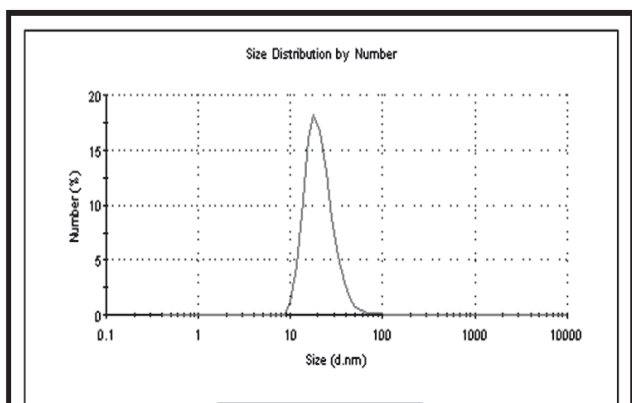


**Fig. 1.** Particle size distribution for silver nanoparticles synthesized by *B. licheniformis*.

ter-insoluble iodinitrotetrazolium formazan (INF); thus, the dehydrogenase activity can be determined by the change of the spectrophotometric value of INF. The dehydrogenase activity was then calculated according to the maximum spectrophotometrical absorbance of INF at 490 nm.

**Detection of reactive oxygen species (ROS).** The ROS formed by AgNPs was identified using 2',7'-dichlorofluorescein diacetate (DCFDA) (Kye et al., 1999). The ROS was detected at 485/20 nm of fluorescence excitation wavelength, and 528/20 nm of emission wavelength using a Fluorescence Multi-Detection Reader.

**Statistical analysis.** All experiments were repeated at least three times. The results were presented as means  $\pm$ SD. All experimental data were compared using the Student's *t*-test. A *p*-value less than 0.05 was considered statistically significant.

## Results and Discussion

### Screening of silver-nanoparticle-producing bacteria

Thirty bacterial strains were isolated from agricultural fields of different localities in Egypt. Screening of silver-nanoparticle-producing bacteria was primarily carried out by observing the color change of the culture supernatant, after mixing with silver nitrate, from pale yellow to dark brown. Only 10% of isolates (3 strains) exhibited dark brown. In order to confirm the formation of silver nanoparticles (AgNPs), the supernatants were monitored by a UV-Vis absorption spectrum in the range of 300–700 nm. Of these, only one isolate showed an absorption peak centered at 420 nm characteristic of AgNPs, and, therefore, it was selected for further study (data not shown). To confirm the identification of the selected isolate, a 16S rRNA gene sequence analysis was performed. The sequence alignment using BLASTN software for the comparison of up to 1,500 bp indicated that the 16S rRNA gene sequence of *Bacillus licheniformis* NM120-17 strain exhibits a high homology (98%) with that of *Bacillus licheniformis* NRRL B-14262.

The characteristic brown color arises due to the excitation of surface plasmon resonance in the silver metal nanoparticles, and provides a convenient signature of their

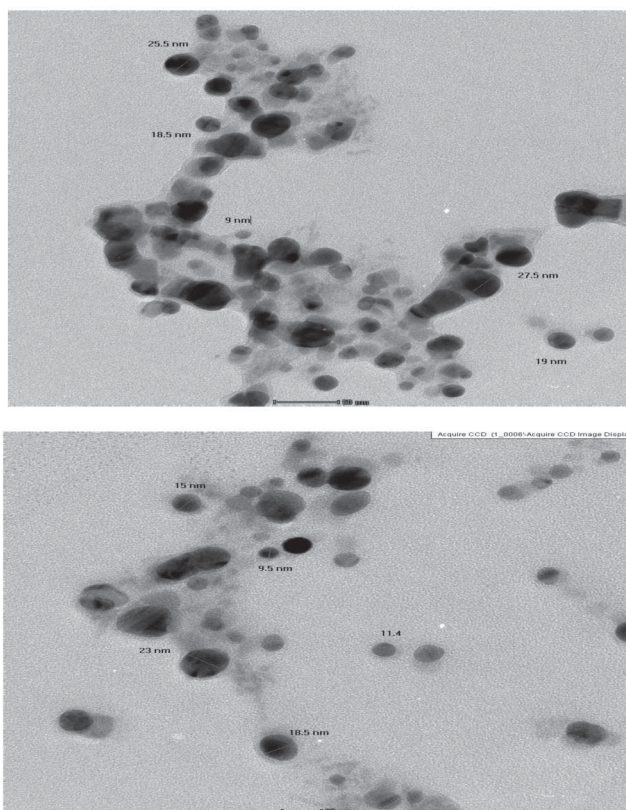


**Fig. 2.** TEM images of silver nanoparticles synthesized by *B. licheniformis*.

Scale bars are 50 nm and 20 nm, respectively. Inset shows the selected area of the diffractometer pattern of the synthesized silver nanoparticles.

formation (El-Naggar et al., 2014). Metal nanoparticles have free electrons, which results in a surface plasmon resonance (SPR) absorption band, due to the combined vibration of electrons of metal nanoparticles in resonance with a light wave. A single surface plasmon resonance (SPR) band corresponds to the spherical nanoparticles, whereas two or more SPR bands correspond to the anisotropic molecules (Pal et al., 2007; Saifuddin et al., 2009). Observation of this sharp clear peak, assigned to a surface plasmon, was well documented for various metal nanoparticles with sizes ranging from 2 to 100 nm (Kowshik et al., 2003).

The biosynthesis of silver nanoparticles by *B. licheniformis* NM120-17 occurred at 24 h, which is quite fast and required less time than previously published strains (Chaudhari et al., 2012; Kalimuthu et al., 2008; Kalishwaralal et al., 2010). An extracellular polymeric substance played a critical role in the reduction of silver ion and nanoparticle stabilization when using the cell-free extract (Padman et al., 2014). The most widely accepted mechanism of silver biosynthesis is the presence of the nitrate reductase enzyme. The enzyme converts nitrate into nitrite and the electron is transferred to the silver ion; hence, the silver ion is reduced to silver ( $\text{Ag}^+$  to  $\text{Ag}^0$ ) (Vaidyanathan et al., 2010). It is worth noting that the pH of the culture supernatant was adjusted to pH 8.5 with NaOH. The alkaline pH increases the synthesis reaction rate as well as favoring the synthesis of smaller-sized nanoparticles (Deepak et al., 2011). Also, under alkaline

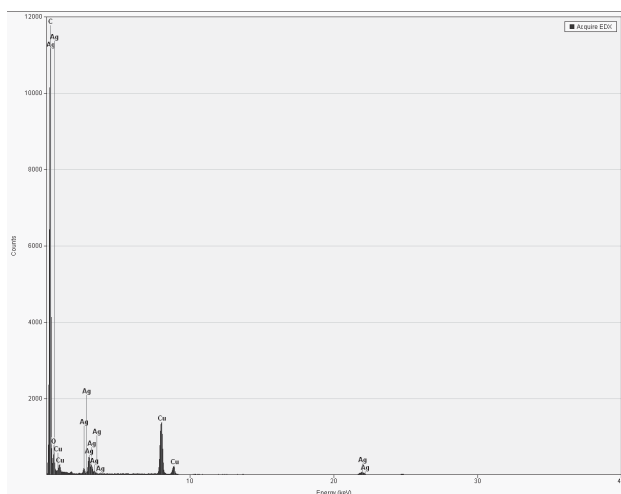


Fig. 3. EDX spectrum of silver nanoparticles synthesized by *B. licheniformis*.

conditions the ability of the enzyme responsible for the synthesis of silver nanoparticles increases.

#### Characterization of silver nanoparticles

**Particle size distribution.** The size distribution by intensity gives a bell-shaped pattern which indicates the wide range size distribution of nanoparticles in the sample formulation as shown in Fig. 1. The size of Ag nanoparticles dispersed was in the range 10.1 nm to 68.06 nm. The average particle size (d 50) is expected to be 18.17 nm.

**Transmission Electron Microscopy (TEM) and Energy Dispersive X-ray Spectra (EDX) analysis.** The morphology, size and distribution of nanoparticles was observed through TEM micrographs (Fig. 2). The morphology of the nanoparticles was spherical in nature and uniformly distributed. The size of the silver nanoparticles ranged from 9–27.5 nm and the average size was estimated to be 17 nm. The presence of elemental silver in the biologically-synthesized nanoparticle solution was confirmed by EDX analysis (Fig. 3) where strong optical absorption peaks were observed at approximately 3 keV, which is typical for the absorption of metallic silver nanocrystallites due to surface plasmon resonance. A few weaker signals from C and O were also recorded which may be due to X-ray emissions from the organism (Mouxing et al., 2006).

**XRD studies.** Analysis through X-ray diffraction was carried out to confirm the crystalline nature of the silver nanoparticles. The XRD pattern showed a number of Bragg reflections that may be indexed on the basis of the face-centered cubic structure of silver. A comparison of our XRD spectrum with the standard confirmed that the silver particles formed in our experiments were in the form of nanocrystals, as evidenced by the three distinct diffraction peaks at  $2\theta$  values of  $30.01^\circ$ ,  $34.50^\circ$ , and  $46.30^\circ$  which are indexed as the (111), (200), and (220) Bragg reflections, respectively, and which can be indexed based on the face-centered cubic structure of silver (Fig. 4). The sharp peaks clearly confirm the crystalline nature of the synthesized nanoparticles which is in good agreement with earlier reports (Anuj and Ishnava, 2013). The unassigned

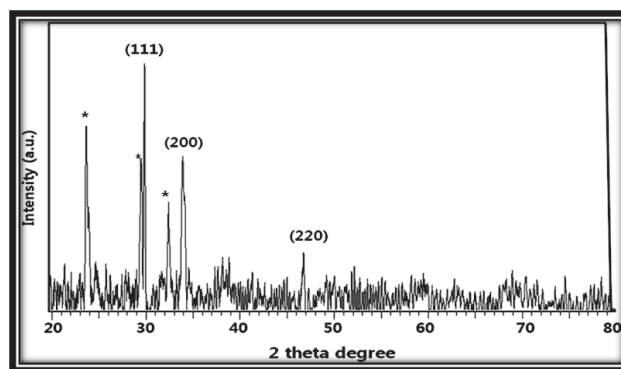


Fig. 4. XRD pattern of silver nanoparticles synthesized by *B. licheniformis*.

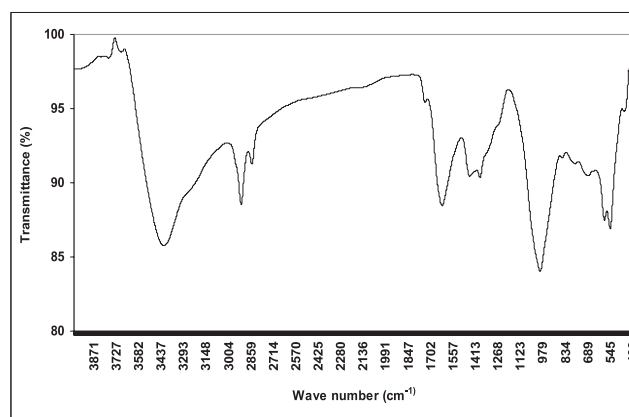


Fig. 5. FTIR spectrum of silver nanoparticles synthesized by *B. licheniformis*.

peaks present in the spectrum, denoted by (\*), indicated the presence of fewer biomolecules of stabilizing agents of enzymes or proteins in the bacterial cell-free extract (Daizy, 2009).

**FT-IR spectroscopy.** FT-IR measurement was carried out to identify the possible biomolecules for capping and the efficient stabilization of the silver nanoparticles synthesized by bacterial broth. The peaks at  $3423$  and  $2924$   $\text{cm}^{-1}$  revealed the presence of an N-H bend, indicating the primary and secondary amine groups of protein (Fig. 5). Likewise, the bands at  $1629$  and  $1453$   $\text{cm}^{-1}$  correspond to the primary and secondary amine groups of N-H bending and the carbonyl stretching vibrations of protein, respectively (Sawle et al., 2008). Therefore, the FTIR study has shown that the carbonyl groups of amino acid residues, as well as the peptides of proteins, have a stronger metal-binding capability (Sathyavati et al., 2010). Most possibly, the proteins could form a coat to cover the nanoparticles and act as capping agents for silver nanoparticle formation to avert the agglomeration of the nanoparticles; thereby stabilizing the particles (Mallikarjuna et al., 2011). Moreover, the band at  $1739$   $\text{cm}^{-1}$  corresponds to C=O stretching vibrations of the aldehyde group. Hence, the observations indicate that the bioreductions of silver nitrate are tied to the oxidation of hydroxyl groups in bacterial cell filtrate (Sangi and Verma, 2009). The entire observations suggest that the biological

**Table 1.** Antibacterial activity of silver nanoparticles produced by *Bacillus licheniformis* against the tested microorganisms.

Bacterial strains	Inhibition zone diameter (mm)			
	<i>B. licheniformis</i> supernatant	AgNO <sub>3</sub>	AgNPs	Streptomycin (positive control)
<i>Bacillus subtilis</i> NCTC10400	—	3 ± 0.2	10 ± 0.12	9 ± 0.11
<i>Bacillus cereus</i> ATCC1589	—	9 ± 0.15	13 ± 0.05	10 ± 0.16
<i>Staphylococcus aureus</i> ATCC29213	—	8 ± 0.13	17 ± 0.16	13 ± 0.01
<i>Klebsiella pneumonia</i> ATCC10031	—	3 ± 0.01	7 ± 0.14	15 ± 0.14
<i>Salmonella typhi</i> NCIMB9331	—	5 ± 0.00	12 ± 0.02	14 ± 0.05
<i>Escherichia coli</i> ATCC10536	—	7 ± 0.31	15 ± 0.3	12 ± 0.00
<i>Pseudomonas aeruginosa</i> ATCC10145	—	6 ± 0.01	9 ± 0.08	17 ± 0.04

Values are means ±SD of 3 separate experiments.

— No inhibition zone.

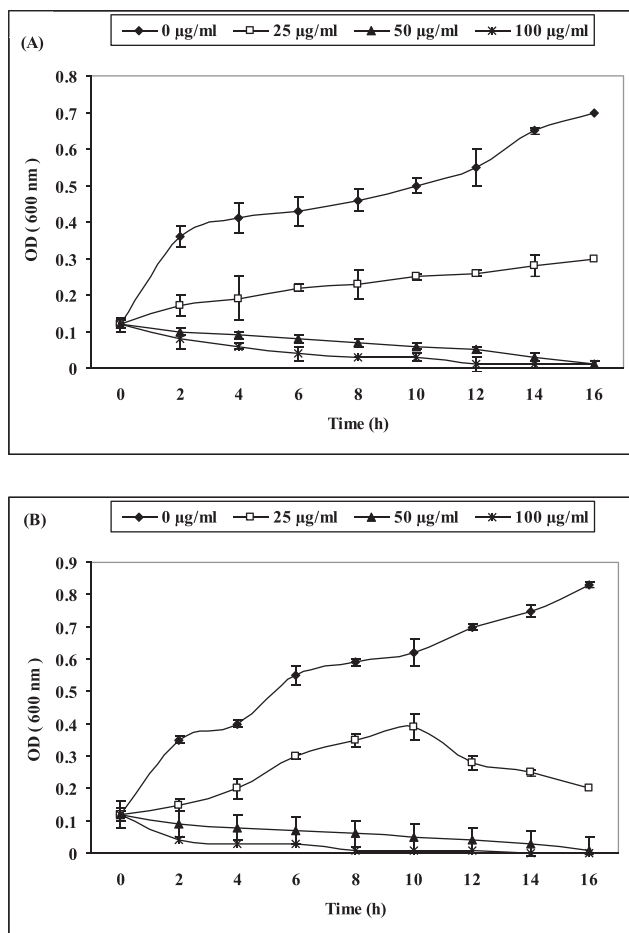


**Fig. 6.** Growth curves of *S. aureus* (A) and *E. coli* (B) cells exposed to different concentrations ( $\mu\text{g/ml}$ ) of AgNPs under normal conditions.

Data are the average from triplicate experiments. Error bars represent standard deviations of triplicate readings.

molecules might possibly be the reason for the formation and stabilization of metal nanoparticles in the bacterial cell filtrate.

**Antibacterial activity of silver nanoparticles.** Silver nanoparticles have been evaluated for their antimicrobial activities against a wide range of pathogenic organisms using the agar well diffusion method. After the incubation time, clear zones were observed against all the test organ-

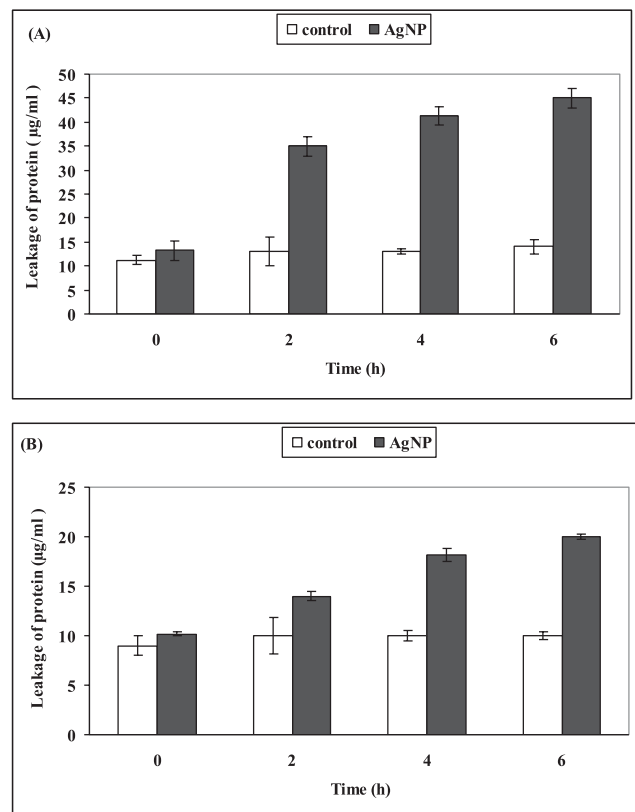


**Fig. 7.** Leakage of protein from *S. aureus* (A) and *E. coli* (B) cells exposed to AgNPs.

The AgNPs group was treated with AgNPs at the concentration of 50  $\mu\text{g/ml}$ , and the control was not treated. The data shown are the average from triplicate experiments. Error bars represent standard deviations of triplicate readings.

isms by AgNPs and were recorded in millimeters (Table 1). The highest sensitivity was observed in the case of *Staphylococcus aureus* (17 mm), followed by *Escherichia coli* (15 mm), then *Bacillus cereus* (13 mm). The efficacy of silver nanoparticles can be attributed to the extremely small size and large surface area relative to their volume (Pal et al., 2007). This indicates that silver nanoparticles have an excellent biocidal effect and potential in reducing bacterial growth in practical applications.

#### **Growth curve of *S. aureus* and *E. coli* exposed to AgNPs**

Growth curves of bacterial cells treated with different

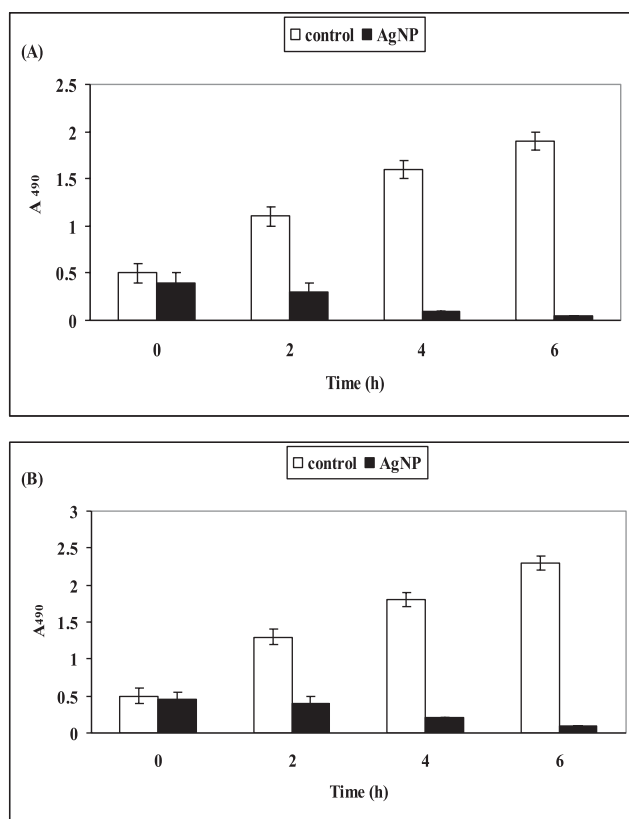


**Fig. 8.** Effect of AgNPs on respiration chain dehydrogenases in *S. aureus* (A) and *E. coli* (B) cells exposed to AgNPs.

The AgNPs group was treated with AgNPs at the concentration of 50  $\mu\text{g/ml}$ , and the control was not treated. The data shown are the average from triplicate experiments. Error bars represent standard deviations of triplicate readings.

concentrations of AgNPs indicated that AgNPs could inhibit the growth and reproduction of bacterial cells (Figs. 6A and B). The bacterial growth of the cells treated with 25 mg/ml AgNPs was slightly lower than that of cells in the control group, whereas the growth of bacterial cells treated with 50 and 100 mg/ml AgNPs were greatly inhibited. Interestingly, upon comparison of the bacterial growth curves, the growth curves of the AgNPs-treated bacteria indicated a faster growth inhibition of *E. coli* than of *S. aureus*. When the concentration of AgNPs was 50 mg/ml, no growth of *S. aureus* and *E. coli* could be detected, indicating that the MIC of AgNPs to *S. aureus* and *E. coli* was 50 mg/ml.

**Effect of AgNPs on the membrane leakage of proteins and reducing sugars.** Results cited in Figs. 7A and B indicated that AgNPs could enhance protein leakage by increasing the membrane permeabilities of *S. aureus* and *E. coli* cells. Initially, protein leakage from the membranes of bacterial cells treated with AgNPs was almost the same as that from cells in the control group. In starting time, the leakage of proteins from cells in the control experiment was 11.23 and 9.0 mg/ml, while leakage of proteins from cells treated with AgNPs was 13.25 and 10.14 mg/ml for *S. aureus* and *E. coli* cells, respectively. The leakage of proteins in *S. aureus* and *E. coli* treated with AgNPs for 4 h was up to 41.28 and 18.16 mg/ml, respectively. At

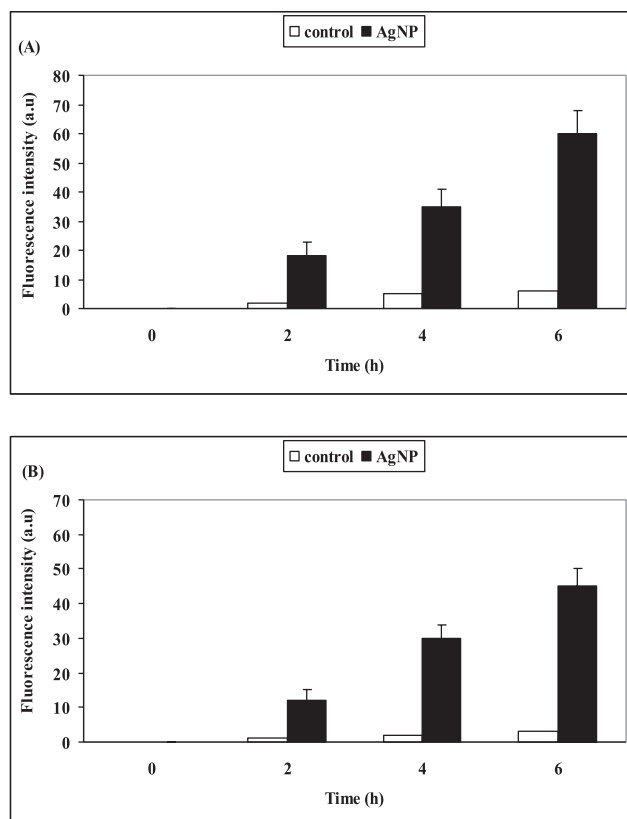


**Fig. 9.** Formation of ROS in *S. aureus* (A) and *E. coli* (B) cells exposed to AgNPs.

The AgNPs group was treated with AgNPs at the concentration of 50  $\mu\text{g/ml}$  for 0 h, 2h, 4h, or 6 h. The data shown are the average from triplicate experiments. Error bars represent standard deviations of triplicate readings.

6 h after incubation, protein leakage from cells treated with AgNPs considerably increased; however, there was no change in the amount of protein leakage from cells in the control group. Notably, higher amounts of proteins leaked through the *S. aureus* membranes compared to those through the *E. coli* membranes, suggesting that the antibacterial sensitivity of the Gram-positive *S. aureus* was higher than that of the Gram-negative *E. coli*.

Furthermore, it is revealed that AgNPs could enhance the membrane leakage of reducing sugars (data not shown). In starting time, almost no reducing sugars could be detected to leak from bacterial cells in the control experiment. After treatment with AgNPs for 6 h, the leakage amount of reducing sugars was up to 100.5 and 60.22 mg/ml, respectively, but was only 40.50 and 20.00 mg/ml in the control experiment. These experimental results showed that AgNPs apparently enhanced the permeability of bacterial cell membranes. So it could be inferred that turbulence of membranous permeability would be an important factor for the inhibition of bacterial growth. But it is still a mystery where the damage takes place, on the lipopolysaccharide or membrane proteins in the outer membrane.

**Effect of AgNPs on the respiratory chain dehydrogenase activity.** The effect of AgNPs on respiration chain dehydrogenase activity of *S. aureus* and *E. coli* cells are shown in Figs. 8A and B. The activity of the enzyme in the con-

tol group increased considerably with time, whereas the activity decreased in the cells treated with AgNPs. These results indicated that the activity of respiratory chain dehydrogenase could be inhibited by AgNPs. It is assumed that AgNPs may break through the barrier of the outer membrane permeability, peptidoglycan and periplasm, and destroy the respiratory chain dehydrogenases, thereby inhibiting the respiration of cells (Li et al., 2010).

**Formation of ROS from bacterial cells treated with AgNPs.** Reactive oxygen species (ROS) are natural by products of the metabolism of respiring organisms. While small levels can be controlled by the antioxidant defenses of the cells such as the glutathione/glutathione disulfide (GSH/GSSG) ratio, an excess ROS production may produce oxidative stress (Nel et al., 2006). The additional generation of free radicals can attack membrane lipids and lead to a breakdown of membrane and mitochondrial function, or cause DNA damage (Mendis et al., 2005). It was reported that the antibacterial activity of AgNPs is related to the formation of free radicals (Kim et al., 2007). Furthermore, the free radicals generated by the AgNPs induce bacterial cell membrane damage. ROS can exist naturally in intracellular and extracellular locations (Danilczuk et al., 2006). Under certain conditions, high levels of ROS can increase oxidative stress in cells. Oxidative stress can not only cause damage to the cell membrane, but can also cause damage to the proteins, DNA, and intracellular systems such as the respiratory system. In this study, ROS was measured using DCFDA. After 6 h incubation, significantly increased production of ROS was detected in the AgNPs-treated group of *S. aureus* and *E. coli*, but not in the control group (Figs. 9A and B). These results indicate that AgNPs can form ROS with water and, hence, the bacterial cell membrane, protein structure and intracellular system can be damaged owing to the ROS formed by AgNPs.

## References

- Akaighe, N., Mac Cusprie, R. I., Navarro, D. A., Aga, D. S., Banerjee, S. et al. (2011) Humic acid-induced silver nanoparticle formation under environmentally relevant conditions. *Environ. Sci. Technol.*, **45**, 3895–3901.
- Altschul, S. F., Thomas, L. M., Alejandro, A. S., Zhang, J., Zhang, Z. et al. (1997) Gapped BLAST and PSI-BLAST, a new generation of protein database search programs. *Nucleic Acids Res.*, **25**, 3389–3402.
- Anuj, S. A. and Ishnava, K. B. (2013) Plant mediated synthesis of silver nanoparticles by using dried stem powder of *Tinospora cordifolia*, its antibacterial activity and comparison with antibiotics. *Int. J. Pharm. Biol. Sci.*, **44**, 849–863.
- Chaudhari, P. R., Masurkar, S. A., Shidore, V. B., and Kamble, S. P. (2012) Effect of biosynthesized silver nanoparticles on *Staphylococcus aureus* biofilm quenching and prevention of biofilm formation. *Int. J. Pharm. Biol. Sci.*, **3**, 222–229.
- Daizy, P. (2009) Biosynthesis of Au, Ag and Au-Ag nanoparticles using edible mushroom extract. *Spect. Acta Part A, Mol. Biomol. Spect.*, **73**, 374–381.
- Danilczuk, M., Lund, A., Saldo, J., Yamada, H., and Michalik, J. (2006) Conduction electron spin resonance of small silver particles. *Spect. Acta Part A, Mol. Biomol. Spect.*, **63**, 189–191.
- Darroudi, M., Ahmad, M. B., Abdullah, A. H., Ibrahim, N. A., and Shamel, K. (2010) Effect of accelerator in green synthesis of silver nanoparticles. *Int. J. Mol. Sci.*, **11**, 3898–3905.
- Deepak, V., Kalishwaralal, K., Pandian, S. R., and Gurunathan, S. (2011) An insight into the bacterial biogenesis of silver nanoparticles, industrial production and scale-up. In *Metal Nanoparticles in Microbiology*, ed. by Rai, M., Duran, N., Berlin, pp. 17–35.
- Dobrucka, R. and Dlugaszewska, J. (2015) Antimicrobial activities of silver nanoparticles synthesized by using water extract of *Arinicae anthodium*. *Ind. J. Microbiol.*, **55**, 168–174.
- Durán, N., Marcato, P. D., Ingle, A., Gade, A., and Rai, M. (2010) Fungi-mediated synthesis of silver nanoparticles, characterization processes and applications. *Prog. Mycol.*, 425–449.
- El-Naggar, N. E., Abdelwahed, N. A. M., and Darwesh, O. M. M. (2014) Fabrication of biogenic antimicrobial silver nanoparticles by *Streptomyces aegyptia* NEAE 102 as eco-friendly nanofactory. *J. Microbiol. Biotechnol.*, **244**, 453–464.
- Gade, A., Bonde, P., Ingle, A. P., Marcato, P. D., Durán, N. et al. (2008) Exploitation of *Aspergillus niger* for synthesis of silver nanoparticles. *J. Biobased Mater. Bioenergy*, **2**, 243–247.
- Gomaa, E. Z. (2012) Chitinase production by *Bacillus thuringiensis* and *Bacillus licheniformis*: their potential in antifungal biocontrol. *J. Microbiol.*, **50**, 103–111.
- Gurunathan, S., Kalishwaralal, K., Vaidyanathan, R., Deepak, V., Pandian, S. R. K. et al. (2009) Biosynthesis, purification and characterization of silver nanoparticles using *Escherichia coli*. *Colloid Surf. B*, **74**, 328–335.
- Iturriaga, R., Zhang, S., Sonek, G. J., and Stibbs, H. (2001) Detection of respiratory enzyme activity in *Giardia* cysts and *Cryptosporidium oocysts* using redox dyes and immunofluorescence techniques. *J. Microbiol. Methods*, **46**, 19–28.
- Kalimuthu, K., Babu, R. S., Venkataraman, D., Bilal, M., and Gurunathan, S. (2008) Biosynthesis of silver nanocrystals by *Bacillus licheniformis*. *Colloid Surf. B*, **65**, 150–153.
- Kalishwaralal, K., Barathmanikant, S., Pandian, S. R. K., Deepak, V., and Gurunathan, S. (2010) Silver nanoparticles impede the biofilm formation by *Pseudomonas aeruginosa* and *Staphylococcus epidermidis*. *Colloid Surf. B*, **79**, 340–344.
- Kim, J. S., Kuk, E., Yu, K. N., Kim, J. H., Park, S. J. et al. (2007) Antimicrobial effects of silver nanoparticles. *Nanomed. Nanotechnol.*, **3**, 95–101.
- Kowshik, M., Ashtaputre, S., Kharrazi, S., Vogel, W., Urban, J. et al. (2003) Extracellular synthesis of silver nanoparticles by a silver-tolerant yeast strain MKY3. *Nanotechnology*, **14**, 95–100.
- Kye, I. S., Jeon, Y. S., No, J. K., Kim, Y. J., Lee, K. H. et al. (1999) Reactive oxygen scavenging activity of green tea polyphenols. *J. Korea Gerontol.*, **9**, 10–17.
- Li, W. R., Xie, X. B., Shi, Q. S., Zeng, H. Y., Ou-Yang, Y. S. et al. (2010) Antibacterial activity and mechanism of silver nanoparticles on *Escherichia coli*. *Appl. Microbiol. Biotechnol.*, **85**, 1115–1122.
- Lowry, O. H., Rosebrough, N., Farr, A. L., and Randall, R. J. (1951) Protein measurement with Folin phenol reagent. *J. Biol. Chem.*, **193**, 265–275.
- Magana, S. M., Quintana, P., Aguilar, D. H., Toledo, J. A., Angeles-Chavez, C. et al. (2008) Antibacterial activity of montmorillonites modified with silver. *J. Mol. Catal. A, Chem.*, **281**, 192–199.
- Mallikarjuna, K., Narasimha, G., Dillip, G. R., Praveen, B., Shreedhar, B. et al. (2011) Green synthesis of silver nanoparticles using ocimum leaf extract and their characterization. *Digest J. Nanomat. Biostruc.*, **6**, 181–186.
- Masurkar, S. A., Chaudhari, P. R., Shidore, V. B., and Kamble, S. P. (2011) Rapid biosynthesis of silver nanoparticles using *Cymbopogon citrates* (lemongrass) and its antimicrobial activity. *Nano. Micro. Lett.*, **3**, 189–194.
- Mendis, E., Rajapakse, N., Byun, H., and Kim, S. (2005) Investigation of jumbo squid *Dosidicus gigas* skin gelatin peptides for their *in vitro* antioxidant effects. *Life Sci.*, **77**, 2166–2178.
- Miller, G. (1959) Use of dinitrosalicylic acid reagent for determination of reducing sugars. *Anal. Chem.*, **31**, 426–429.
- Mouying, F. U., Qingbiao, L. I., Daohua, S. U. N., Yinghua, L. U., Ning, H. E. et al. (2006) Rapid preparation process of silver nanoparticles by bioreduction and their characterisation. *Chinese J. Chem. Eng.*, **141**, 114–117.
- Narayanan, K. and Sakthivel, N. (2010) Biological synthesis of metal nanoparticles by microbes. *Adv. Colloid Interface Sci.*, **153**, 1–13.
- Nel, A., Xia, T., Madler, L., and Li, N. (2006) Toxic potential of materials at the nanolevel. *Science*, **311**, 622–627.

- Padman, A. J., Henderson, J., Hodgson, S., and Rahman, K. S. M. (2014) Biomediated synthesis of silver nanoparticles using *Exiguobacterium mexicanum*. *Biotechnol. Lett.*, **36**, 2079–2084.
- Pal, S., Tak, Y. K., and Song, J. M. (2007) Does the antibacterial activity of silver nanoparticles depend on the shape of the nanoparticle? A study of the gram-negative bacterium *Escherichia coli*. *Appl. Environ. Microbiol.*, **276**, 1712–1720.
- Perez, C., Paul, M., and Bazerque, P. (1990) Antibiotic assay by agar well diffusion method. *Acta Biol. Med. Exp.*, **15**, 113–115.
- Peterson, M. S. M., Bouwman, J., Chen, A., and Deutsch, M. (2007) Inorganic metallo-dielectric materials fabricated using two single-step methods based on the Tollen's process. *J. Colloid Interface Sci.*, **306**, 41–49.
- Raut, R., Lakkakula, J. R., Kolekar, N., Mendhulkar, V. D., and Kashid, S. B. (2010) Extracellular synthesis of silver nanoparticles using dried leaves of *Pongamia pinnata* (*L*) *pirre*. *Nano Micro. Lett.*, **2**, 106–113.
- Rochelle, P. A., Will, J. A. K., Fry, J. C., Jenkins, G. J. S., Parkes, R. J. et al. (1995) Extraction and amplification of 16S rRNA genes from deep marine sediments and seawater to assess bacterial community diversity. In *Nucleic Acids in the Environment*, ed. by Trevors, J. T. and van Elsas, J. D., Springer, Berlin, pp. 219–239.
- Saifuddin, N., Wong, C. W., and Nuryasumira, A. A. (2009) Rapid biosynthesis of silver nanoparticles using culture supernatant of bacteria with microwave irradiation. *E-J. Chem.*, **6**, 61–70.
- Sangi, R. and Verma, P. (2009) Biomimetic synthesis and characterization of protein capped silver nanoparticles. *Bioresour. Technol.*, **100**, 501–504.
- Sathyavati, R., Krishna, M. B., Rao, S. V., Saritha, R., and Rao, D. N. (2010) Biosynthesis of silver nanoparticles using *Coriandrum sativum* leaf extract and their application in nonlinear optics. *Adv. Sci. Lett.*, **31**, 138–143.
- Sawle, B. D., Salimath, B., Deshpande, R., Bedre, M. D., Prabhakar, B. K. et al. (2008) Biosynthesis and stabilization of Au and Au-Ag alloy nanoparticles by fungus *Fusarium semitectum*. *Sci. Technol. Adv. Mater.*, **9**, 35–42.
- Schaller, M., Laude, J., Bode, H., Hamm, G., and Korting, H. C. (2004) Toxicity and antimicrobial activity of a hydrocolloid dressing containing silver particles in an *ex vivo* model of cutaneous infection. *Skin Pharmacol. Physiol.*, **17**, 31–36.
- Shao, K. and Yao, J. (2006) Preparation of silver nanoparticles via a non-template method. *Mater. Lett.*, **60**, 3826–3829.
- Souza, G. I. H., Marcato, P. D., Durn, N., and Esposito, E. (2004) Utilization of *Fusarium oxysporum* in the biosynthesis of silver nanoparticles and its antibacterial activities. In IX National Meeting of Environmental Microbiology, Curitiba PR Brazil.
- Tomsic, B., Simoncic, B., Orel, B., Zerjav, M., and Schroers, H. J. (2009) Antimicrobial activity of AgCl embedded in a silica matrix on cotton fabric. *Carbohydr. Polym.*, **75**, 618–626.
- Tsuji, T., Iryo, K. N., Watanabe, N., and Tsuji, M. (2002) Preparation of silver nanoparticles by laser ablation in solution, influence of laser wavelength on particle size. *Appl. Surf. Sci.*, **202**, 80–85.
- Vaidyanathan, R., Gopalram, S., Kalishwaralal, K., Deepak, V., Pandian, S. R. et al. (2010) Enhanced silver nanoparticle synthesis by optimization of nitrate reductase activity. *Colloids Surf. B. Biointerfaces*, **75**, 335–341.
- Vigneshwaran, N., Ashtaputre, N. M., Varadarajan, P. V., Nachane, R. P., Paralikar, K. M. et al. (2007) Biological synthesis of silver nanoparticles using the fungus *Aspergillus flavus*. *Mater. Lett.*, **61**, 1413–1418.
- Wang, X. F., Li, S. F., Yua, H. G., and Yu, J. G. (2011) *In situ* anion exchange synthesis and photocatalytic activity of Ag<sub>8</sub>W<sub>4</sub>O<sub>16</sub>/AgCl-nanoparticle core-shell nanorods. *J. Mol. Catal. A. Chem.*, **334**, 52–59.
- Wani, I. A., Khatoon, S., Ganguly, A., Ahmed, J., and Ahmad, T. (2013) Structural characterization and antimicrobial properties of silver nanoparticles prepared by inverse microemulsion method. *Colloid Surf. B*, **101**, 243–250.